



ELSEVIER

Available online at www.sciencedirect.com

SCIENCE @ DIRECT®

Journal of Magnetism and Magnetic Materials 286 (2005) 206–210

Journal of
magnetism
and
magnetic
materials

www.elsevier.com/locate/jmmm

Magnetization reversal of ferromagnetic layer in exchange coupled Mn–Ir/Co–Fe epitaxial bilayers

Takashi Sato^a, Masakiyo Tsunoda^{a,*}, Migaku Takahashi^{a,b}

^a*Department of Electronic Engineering, Tohoku University, Aobayama 05, Sendai 980-8579, Japan*

^b*New Industry Creation Hatchery Center, Tohoku University, Sendai 980-8579, Japan*

Available online 21 October 2004

Abstract

The magnetization reversal process for Mn–Ir/Co–Fe epitaxial bilayers was investigated using magneto-optical Kerr microscopy. It was found that the magnetization reversal of the ferromagnetic layer progresses in different ways when the crystallographic orientation of the bilayers is changed. In the (1 1 0) bilayers, 180° domain walls sweep over the whole film plane to reverse the magnetization of the ferromagnetic layer. On the other hand, in (0 0 1) bilayers, smaller domains nucleated homogeneously in the film plane combine with each other around the coercive fields and saturate the magnetization.

© 2004 Elsevier B.V. All rights reserved.

PACS: 75.60.Jk; 75.70.Cn; 75.30.Gw

Keywords: Spin valve; Co–Fe; Mn–Ir; Directional control; Magnetization reversal; Domain pattern

1. Introduction

An understanding of the exchange anisotropy of ferromagnetic (FM)/antiferromagnetic (AFM) bilayers is of great interest due to their applications in magnetoelectronic devices based on the giant- and tunnel-magnetoresistive effects. Applications in hard disk drives (HDDs) which need to provide a fixed magnetization direction in one of two FM layers of spin valves (SVs) are currently facing a

crucial situation. Dimensions of SV elements continue to decrease in size, and will be comparable to typical thin film grain diameters in the near future, if the current rate of increase in areal recording density of HDDs is maintained. In such cases, an SV element is composed of a single crystal and its magnetic/transport properties might be different from those of the present polycrystalline SVs. One of the issues regarding the exchange anisotropy that should be discussed for the forthcoming single crystalline nano-scaled SVs is the magnetization process of the exchange biased FM layer. Magnetic domain observation is useful for

*Corresponding author. Fax: +81 22 263 9416.

E-mail address: tsunoda@ecei.tohoku.ac.jp (M. Tsunoda).

directly determining the magnetization process of an FM layer and many works on Mn–Ir/Co–Fe bilayer systems using Lorentz microscopy [1–4] and Kerr microscopy [5–7] have been reported. However, these investigations were limited to bilayers with crystallographic random or out-of-plane fiber-textured orientations, and were not applied to the single crystalline bilayers. We thus investigate the magnetization reversal process of an FM layer by magneto-optical Kerr (MOKE) microscopy, using pseudo-single crystalline Mn–Ir/Co–Fe bilayers with different crystallographic orientations.

2. Experimental procedure

Exchange-coupled bilayers with a substrate/buffer layer/Mn₇₅Ir₂₅ d_{AF} /Co₇₀Fe₃₀ 2 nm/Ni–Fe 5 nm structure were deposited on MgO single crystal substrates with crystallographic orientations of either (110) or (001) at room temperature. A DC magnetron sputtering machine with an ultimate pressure less than 5×10^{-9} Torr was used. In order to achieve the epitaxial growth of bilayers on the MgO substrates, a 20 nm-thick Cu buffer layer was inserted [8]. The 5 nm-thick Ni–Fe layer was used to obtain large Kerr signals from the FM layer. A magnetic field of 30 Oe was applied during the deposition of the bilayers, parallel to the film plane along MgO[1 $\bar{1}$ 0] for (110) substrates and along MgO[1 0 0] for (001) substrates. After the deposition, the specimens were annealed at 240 °C for 0.5 h under a vacuum of less than 3×10^{-6} Torr, with an applied magnetic field of 1 kOe along the same direction as that of the field applied during the deposition. The d_{AF} was changed to 0 (without AFM layer), 2, and 5 nm. The obtained epitaxial relationships, determined by X-ray diffraction, were MgO(110)∥Cu(110)∥Mn–Ir(110)∥Co–Fe(211) and MgO[001]∥Cu[001]∥Mn–Ir[001]∥Co–Fe[1 $\bar{1}$ 0] for (110) bilayers, and MgO(001)∥Cu(001)∥Mn–Ir(001)∥Co–Fe(001) and MgO[100]∥Cu[100]∥Mn–Ir[100]∥Co–Fe[110] for (001) bilayers. The Co–Fe layers had a body-centered cubic structure.

The magnetization curves (MH loops) were measured using a vibrating sample magnetometer

(VSM). The unidirectional anisotropy constant, J_K , was calculated using the equation, $J_K = M_s d_F H_{ex}$, where $M_s d_F$ is the areal saturation magnetization of the FM layer, and H_{ex} is the exchange biasing field determined as a shift of the center of the MH loops along the field axis. Domain patterns of the FM layer were observed using MOKE microscopy based on the longitudinal Kerr effect [9] in a magnetic field up to ± 2 kOe. All measurements were performed at room temperature.

3. Results and discussion

The changes in the MH loops of the bilayers with the respective crystallographic orientations as a function of the d_{AF} , are shown in Fig. 1. The external field, H , was applied along MgO[1 $\bar{1}$ 0] for the (110) bilayers and along MgO[1 0 0] for the (001) bilayers. When the $d_{AF} = 0$, magnetization of the FM layer reverses symmetrically in a low field for both the bilayers. The coercive field is 17 and 10 Oe for the (110) and (001) bilayers, respectively. On the other hand, when the

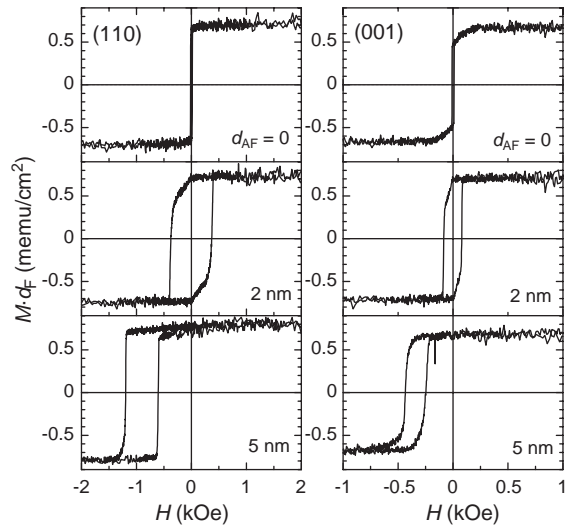


Fig. 1. Magnetization curves of Mn–Ir d_{AF} /Co–Fe 2 nm/Ni–Fe 5 nm epitaxial bilayers with different crystallographic orientations. The external field, H , was applied along MgO[1 $\bar{1}$ 0] for (110) bilayers (left column) and along MgO[1 0 0] for (001) bilayers (right column).

$d_{AF}=2$ nm, the MH loops are still symmetrical to the external applied field, but their coercivity is enhanced remarkably. In contrast, for the bilayers with $d_{AF}=5$ nm, shifted MH loops are observed. This critical phenomenon that depends on the d_{AF} is known as the critical thickness of the exchange anisotropy. Regardless of the crystallographic orientation, the critical thickness, beyond which an exchange bias field appears, is reported as ~ 3 nm for Mn–Ir/Co–Fe epitaxial bilayers when measured at room temperature [8]. The J_K values, determined from the MH loops of the bilayers with $d_{AF}=5$ nm, which were 0.72 erg/cm² for the (110) bilayer and 0.24 erg/cm² for the (001) bilayer, also correspond well with those reported in the previous work [8]. The loop shape near the coercive field is fairly steep for the (110) bilayers, regardless of the d_{AF} . This implies that the magnetization reversal of the FM layer in the (110) bilayers progresses by smooth domain wall motion. On the other hand, the MH loop of the (001) bilayer with $d_{AF}=5$ nm shows a relatively rounded shape around the coercive field, while those of the (001) bilayers with d_{AF} values less than or equal to 2 nm show steep magnetization reversal. This may be due to the different magnetization reversal mechanism from that of the (110) bilayers.

Fig. 2 shows domain images observed around the coercive fields of the (110) bilayers for the different d_{AF} values. Fig. 3 shows the results for the (001) bilayers. The direction of the applied field is also parallel to MgO[110] for the (110) bilayers and to MgO[100] for the (001) bilayers. In both these figures, the left column shows the domain patterns around the coercive field when the applied field is swept from $+H$ to $-H$, corresponding to the MH loops in Fig. 1. The right column shows the domain patterns around the other coercive field. In the case of the single-layered FM ($d_{AF}=0$ cases; Figs. 2a,b and 3a,b), large domains with sharp contrast are observed, regardless of the crystallographic orientation. One of the domains moved along the applied field axis and spread across the field of view of the MOKE microscope when the external applied field was changed slightly. Judging from the contrast change during the field sweep, the observed domain walls

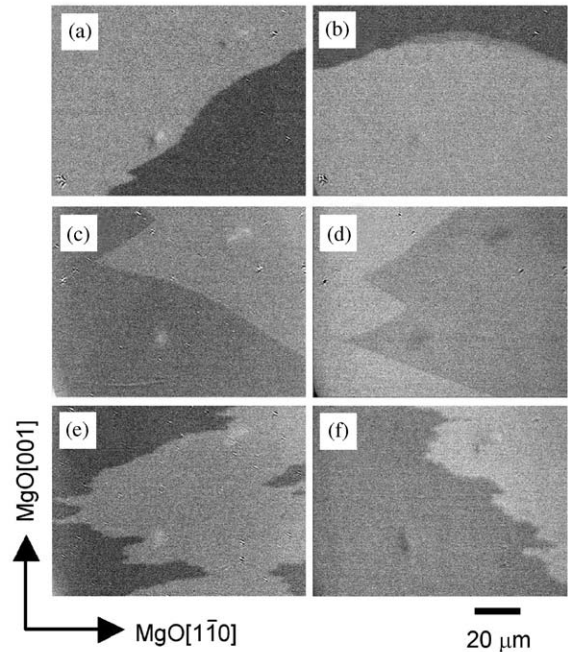


Fig. 2. Domain patterns of (110)-oriented Mn–Ir d_{AF} /Co–Fe 2 nm/Ni–Fe 5 nm epitaxial bilayers around the coercive fields. The d_{AF} is 0 (a,b), 2 nm (c,d), and 5 nm (e,f), respectively. The external field was applied along MgO[110].

are considered to be 180° walls. Large domains with clear contrast were also observed for the (110) bilayers with $d_{AF}=2$ nm (Figs. 2c,d) and 5 nm (Figs. 2e,f). The domain wall motion of the bilayer with $d_{AF}=2$ nm was similar to that for the single-layered FM mentioned above. On the other hand, the domain wall motion of the exchange biased FM layer ($d_{AF}=5$ nm) is somewhat complicated. In general, the domain wall spread across the field of view along the applied field axis as in the above cases, but the shape of the moving wall tended to be a zigzag rather than the straight shape shown in the $d_{AF}=0$ and 2 nm bilayers. Sometimes the wall captured small, newly nucleated domains at the front of the moving wall.

In contrast to the above, the domain patterns of the (001) bilayers with $d_{AF}=2$ nm shown in Figs. 3(c) and (d) clearly indicate a different magnetization reversal process. This process is dominated by the nucleation of many small domains. When the applied field approached the coercive field, many

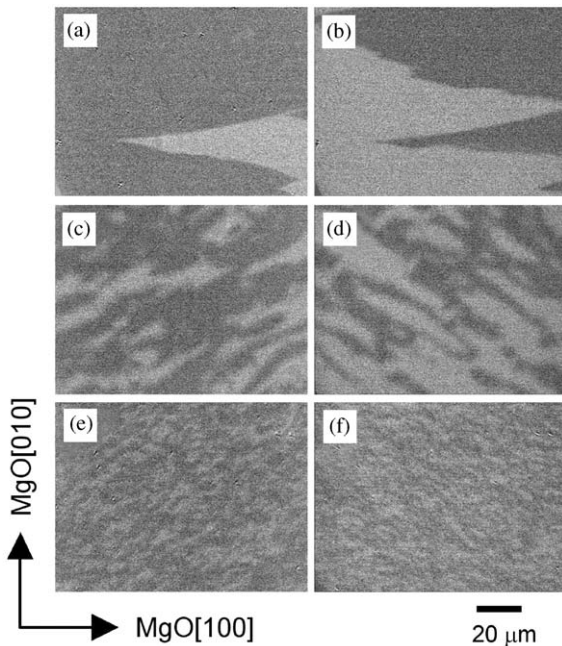


Fig. 3. Domain patterns of (001)-oriented Mn–Ir d_{AF} /Co–Fe 2 nm/Ni–Fe 5 nm epitaxial bilayers around the coercive fields. The d_{AF} is 0 (a,b), 2 nm (c,d), and 5 nm (e,f), respectively. The external field was applied along MgO[100].

small domains appeared homogeneously over the whole field of view of the MOKE microscope. The contrast of these small domains is less than that of the large domains observed in the $d_{AF}=0$ cases. The small domains grew promptly and combined with each other as the applied field was changed slightly. In the case of the (001) bilayer with $d_{AF}=5$ nm, magnetization reversal progressed similarly, except for the much smaller domain size (see Figs. 3e,f). The smaller contrast of the small domains (Figs. 3c–f) in comparison to that of the large domains observed in the (110) bilayers (Figs. 2c–f) or the bilayers with $d_{AF}=0$ (Figs. 2a, b and 3a, b) is probably due to the difference in the relative angle of the magnetization vectors. Taking into account the elongated domain shape of (001) bilayers with finite d_{AF} along $\pm 45^\circ$ from the applied field axis (Figs. 3c–f), we are confident that the magnetization vectors of the small domains align along the respective MgO $\langle 110 \rangle$ direction and that the domain walls observed in Figs. 3c–f are 90° walls.

According to the magneto-torquemetry analysis of the exchange coupled Mn–Ir/Co–Fe epitaxial bilayers having thinner d_{AF} values than the critical thickness, the easy magnetization axes in the film plane are along MgO $\langle 110 \rangle$ for (110) bilayers and along MgO $\langle 110 \rangle$ for (001) bilayers [8]. This might be the cause of the different magnetization reversal processes that take place in the exchange coupled epitaxial bilayers with different crystallographic orientations. Namely, four-fold symmetry of the easy magnetization axis in the (001) bilayer allows the formation of 90° walls in the FM layer, while the two-fold symmetry in the (110) bilayer is responsible for the 180° walls.

4. Summary

Magnetization reversal in Mn–Ir/Co–Fe epitaxial bilayers was investigated using MOKE microscopy. It was found that the magnetization reversal process of the FM layer differs significantly according to the crystallographic orientation of the bilayers. While the 180° domain wall, which separates large domains, sweeps over to reverse the whole magnetization of the ferromagnetic layer in (110) bilayers, small domains are homogeneously nucleated over the whole film plane and are combined with each other to reverse the magnetization in (001) bilayers.

Acknowledgements

The authors are grateful to K. Akahane and S. Meguro of NeoArk Co. Ltd. for their technical support for domain observation.

References

- [1] J.P. King, J.N. Chapman, M.F. Gillies, J.C.S. Kools, *J. Phys. D* 34 (2001) 528.
- [2] Y.G. Wang, A.K. Petford-Long, T. Hughes, H. Laidler, K. O'Grady, M.T. Kief, *J. Magn. Mater.* 242–245 (2002) 1073.
- [3] Y.G. Wang, A.K. Petford-Long, *J. Appl. Phys.* 92 (2002) 6699.

- [4] P. Gogol, J.N. Chapman, M.F. Gillies, F.W.M. Vanhelmont, *J. Appl. Phys.* 92 (2002) 1458.
- [5] Z. Qian, M. Kief, P. George, J. Sivertsen, J. Judy, *J. Appl. Phys.* 85 (1999) 5525.
- [6] J. McCord, R. Schäfer, R. Mattheis, K.-U. Barholz, *J. Appl. Phys.* 93 (2003) 5491.
- [7] R. Seidel, O. de Haas, R. Schaefer, L. Schultz, M. Ruehrig, J. Wecker, *IEEE Trans. Magn.* 38 (2002) 2776.
- [8] T. Sato, M. Tsunoda, M. Takahashi, *J. Appl. Phys.* 95 (2004) 7113.
- [9] K. Akahane, T. Kimura, Y. Ohtani, *J. Magn. Soc. Jpn.* 28 (2004) 2.